Continuum percolation of congruent overlapping spherocylinders

Wenxiang Xu,[1,2,*] Xianglong Su,[1] and Yang Jiao[3,†]

[1] *Institute of Soft Matter Mechanics, College of Mechanics and Materials, Hohai University, Nanjing 211100, People's Republic of China*

[2] *State Key Laboratory of Simulation and Regulation of Water Cycle in River Basin, China Institute of Water Resources and Hydropower Research, Beijing 100048, People's Republic of China*

[3] *Materials Science and Engineering, Arizona State University, Tempe, Arizona 85287, USA*

(Received 3 July 2016; revised manuscript received 24 August 2016; published 20 September 2016)

Continuum percolation of randomly orientated congruent overlapping spherocylinders (composed of cylinder of height H with semispheres of diameter D at the ends) with aspect ratio $\alpha = H/D$ in $[0,\infty)$ is studied. The percolation threshold ϕ_c, percolation transition width Δ, and correlation-length critical exponent ν for spherocylinders with α in [0, 200] are determined with a high degree of accuracy via extensive finite-size scaling analysis. A generalized excluded-volume approximation for percolation threshold with an exponent explicitly depending on both aspect ratio and excluded volume for arbitrary α values in $[0,\infty)$ is proposed and shown to yield accurate predictions of ϕ_c for an extremely wide range of α in [0, 2000] based on available numerical and experimental data. We find ϕ_c is a universal monotonic decreasing function of α and is independent of the effective particle size. Our study has implications in percolation theory for nonspherical particles and composite material design.

DOI: 10.1103/PhysRevE.94.032122

I. INTRODUCTION

Continuum percolation in particle systems, at which a system-spanning cluster emerges, underlies a wide spectrum of material behaviors, such as conduction and flow in porous materials, metal-insulator transition in condensed matter systems, structure of liquid and glasses, and aggregation and self-assembly of colloids [1]. In the vicinity of the percolation threshold, characterized by the critical number density or covering fraction of the particles, dramatic changes of mechanical and transport properties can occur, due to the emergence of global structural connectivity in the system [2,3]. Understanding the nature of percolation transition and accurately predicting the percolation threshold are fundamental and central tasks in the study of continuum percolation of hard or overlapping particle systems [4–6]. The preponderance of previous investigations focused on isotropic particles (e.g., spheres or hyperspheres) [7–9] and recently certain families of nonspherical particles were studied [9–14].

Continuum percolation of spherocylinders, especially the prediction of percolation threshold, has attracted appreciable attention, mainly due to the wide applications of spherocylinder systems in modeling liquid crystals, porous media, nanocomposites of carbon allotropes, fiber-reinforced materials, cellulose whiskers, and silicate nanorods, to name but a few [10–14]. Specifically, theoretical approximations of the percolation threshold based on the Ornstein-Zernike equation for hard spherocylinders [11,13–15] and rigorous bounds [16] have been derived. Numerical simulations of "cherry-pit" spherocylinders consisting of a hard core with an overlapping shell [17–19] have been carried to estimate the percolation threshold. Balberg *et al.* [20] numerically obtained the percolation threshold represented as the critical number density N_c of overlapping sticks in a fixed unit cubic domain. In spite of the aforementioned developments, the finite-size scaling (FSC) behaviors in systems of overlapping spherocylinders with arbitrary aspect ratio have not been systematically investigated. Such FSC analysis is crucial to obtaining an accurate estimate of the percolation threshold in the infinite-size limit and insights of the nature of the percolation transition [20–23].

In this paper, we present a comprehensive finite-size scaling analysis of the continuum percolation of randomly orientated congruent overlapping spherocylinders in a periodic cubic domain using extensive simulations. The percolation threshold ϕ_c, percolation transition width Δ, and correlation-length critical exponent ν for spherocylinders with α in [0, 200] are determined. In addition, a generalized excluded-volume approximation for percolation threshold with an aspect-ratio-dependent exponent is proposed that can accurately predict ϕ_c of overlapping spherocylinders with arbitrary aspect ratios α in $[0,\infty)$. The effect of particle size on ϕ_c is also systematically investigated. We find ϕ_c is a universal monotonic decreasing function of α and is independent of the effective particle size.

II. METHODS

We first generate realizations of congruent overlapping (fully penetrable) spherocylinders of a fixed size with a volume (covering) fraction ϕ in a cubic domain of size L, by randomly placing N spherocylinders in the domain with random orientations [see Fig. 1(a)], i.e., the random sequential addition (RSA) process. We note in this process the particle positions and orientations are totally uncorrelated and follow the Poisson distribution. The particle number N is determined by $N = L^3 \ln(1-\phi)^{-1}/V$ [24], where V is the volume of a particle. For a given volume fraction ϕ, a large number of realizations are generated, and each is checked for percolation as described below. Then the percolation probability, defined as the fraction of percolated realizations for a given volume fraction, is computed as a function of ϕ, from which the percolation threshold can be obtained.

*xwxfat@gmail.com

†yang.jiao.2@asu.edu

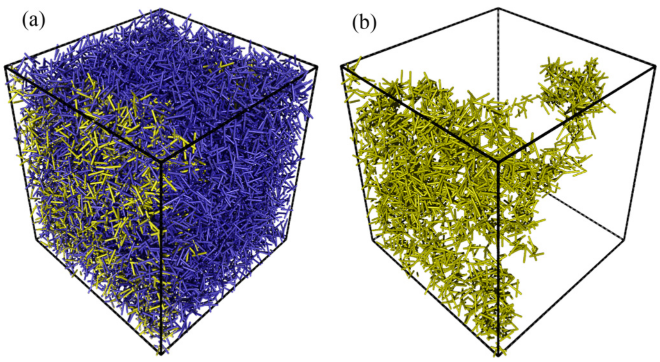

FIG. 1. (a) Realization of a congruent overlapping spherocylinder system with the aspect ratio of $\alpha = 8$; (b) identification of a percolating cluster in the system.

Following Ref. [25], the size of a spherocylinder is characterized by an equivalent radius R_{eq}, which is defined as the radius of an equivalent sphere having the same volume as the spherocylinder. This is a more meaningful length scale for the elongated particle than both the length and semispherical cap radius in the large aspect ratio limit. Accordingly, for a spherocylinder with volume $V = 4\pi R_{\mathrm{eq}}^3/3$, the diameter D of its semispherical cap can be easily computed from the relation $R_{\mathrm{eq}} = 0.5D(1 + 1.5\alpha)^{1/3}$, where α is the aspect ratio of the spherocylinder defined as $\alpha = H/D$, and H is the height of the cylinder part.

The overlap between two spherocylinders is checked by comparing the nearest distance d_{ij} between the axes of symmetry of the spherocylinders with the sum of their radii $(R_i + R_j)$. If $d_{ij} > (R_i + R_j)$, the two spherocylinders do not overlap; otherwise, they overlap [25]. Subsequently, a percolating cluster is identified as one that continuously spans the entire cubic domain from one boundary to an opposite boundary and the spanning ends must overlap under periodic boundary conditions, namely, the "wrapping criterion" is applied [(see Fig. 1(b)], by using a "tree-burning" algorithm [26]. The spanning (percolation) probability $P(\phi, L)$ is then obtained at the volume fraction ϕ of overlapping spherocylinders by averaging over n realizations, following the procedure used in lattice percolation [27,28].

III. RESULTS

A. Finite-size scaling analysis

Here, we present the percolation threshold in terms of the critical volume fraction ϕ_c of spherocylinders, instead of the critical number density N_c or the critical reduced density η_c used in the literature [16–19,27], which can be easily computed from ϕ_c, i.e., $\eta_c = N_c\langle V\rangle$ and $\phi_c = 1 - e^{-\eta_c}$ [2], where $\langle V\rangle$ is the average volume of particles. The percolation threshold ϕ_c characterizes the critical state of emergence of a system-spanning cluster in the infinite-size limit. Thus, it is impossible to directly measure ϕ_c from finite system simulations. The scaling relationship between ϕ_c and the critical volume fraction of $\phi_c(L)$ for the finite systems of size L has been identified [27–29], i.e.,

$$\phi_c(L) - \phi_c \propto L^{-1/\nu}, \tag{1}$$

where ν is the correlation-length critical exponent [29–31], which is rarely studied for the continuum percolation of overlapping spherocylinders. The critical volume fraction $\phi_c(L)$ (also referred to as the effective percolation threshold in Ref. [29]) is generally a particle size- and shape-dependent quantity due to finite-size effects. It is clear that once $\phi_c(L)$ and ν are determined, ϕ_c can be estimated using Eq. (1).

We now derive $\phi_c(L)$ and ν from Monte Carlo (MC) simulations. We first obtain the curve of $P(\phi, L)$-ϕ for a finite system of size L, which possesses a sigmoidal shape, as shown in Fig. 2. The detailed analysis of the percolation probability P as a function of volume fraction ϕ for different aspect ratio α and system size L is shown in Fig. 3. Note that we assign L to be at least 30 times R_{eq} (e.g., $L \geqslant 30R_{\mathrm{eq}}$) so that each realization contains a sufficiently large number of particles for robust statistical analysis. In addition, we employ the coefficient of variation CV associated with $P(\phi, L)$ as a criterion for determining the number of realizations n (e.g., $CV = 0.0004$) [32]. The condition $P(\phi, L) = 0.5$ is used to determine the critical volume fraction of $\phi_c(L)$ for the finite system [17–24,26–29]. In order to accurately determine $\phi_c(L)$ numerically, we use the hyperbolic tangent function (or Gauss error function) [22] to fit the curve of P-ϕ (see Fig. 1), i.e.,

$$P(\phi, L) = \frac{1}{2}\left\{1 + \tanh\left[\frac{\phi - \phi_c(L)}{\Delta(L)}\right]\right\}, \tag{2}$$

where Δ characterizes the width of the percolation transition.

Figure 4(a) shows Δ for different α as a function of system size L. It can be seen that Δ is a particle size- and shape-dependent quantity, which decreases with increasing L and α. For different α, the curves of Δ-L are approximately parallel to one another, which is consistent with the previous study on overlapping spheres [29]. On the other hand, according to the scaling relation between Δ and ν [see Eq. (3)], the value of ν can be obtained as follows:

$$\Delta(L) \propto L^{-1/\nu}. \tag{3}$$

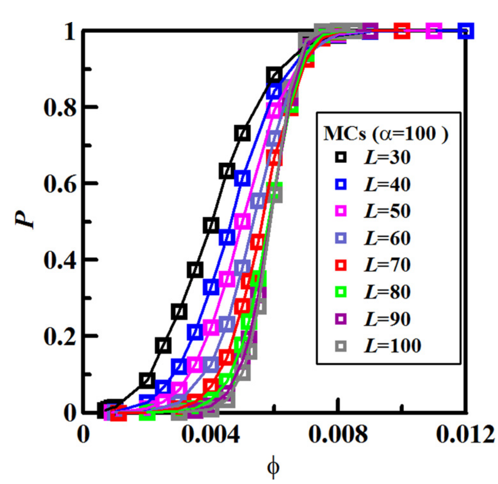

FIG. 2. Percolation probability P for different sizes L of cubic domain as a function of ϕ for congruent overlapping spherocylinders. The parameters of the particles are $R_{\mathrm{eq}} = 1.0$ and $\alpha = 100.0$. The cubic symbols are MC simulation results and the lines are fitting results. The percolation probability curves for various α are displayed in Fig. 3.

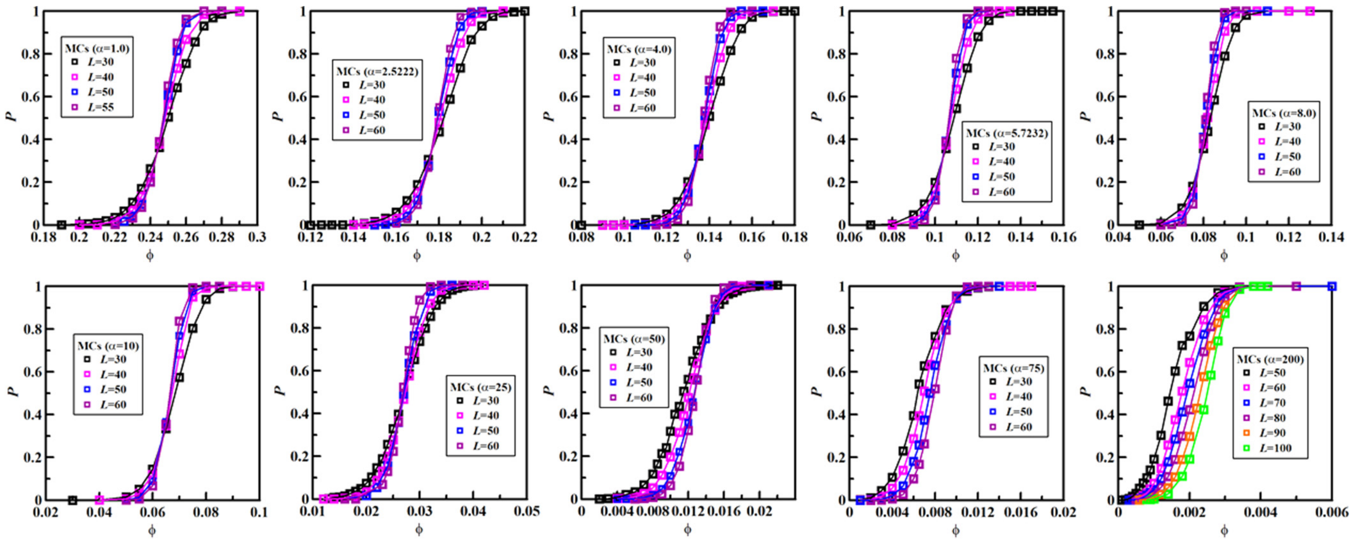

FIG. 3. Percolation probability $P(\phi,L)$ versus ϕ for different α and system sizes of L. The cubic symbols are MC simulation results and the lines are fitting results. The parameters of the particles are $R_{\mathrm{eq}} = 1.0$.

After deriving $\phi_c(L)$ and ν, the percolation threshold ϕ_c is subsequently estimated from the scaling relation (1), as shown in Fig. 4(b). According to the scaling law (1), the interception of each $\phi_c(L)$-$L^{-1/\nu}$ curve with the y axis provides the corresponding effective percolation threshold associated with $L = \infty$, namely, the percolation threshold ϕ_c for the infinite system. From a linear fit to the data for $\alpha = 0$ (i.e., spheres) in Fig. 4(b), we obtain $\phi_c = 0.2896 \pm 0.0007$ for overlapping spheres. This value is consistent with the simulated results from Rintoul and Torquato ($\phi_c = 0.2895 \pm 0.0005$) [29] and Ziff and co-workers ($\phi_c = 0.289\,572\,978 \pm 0.000\,005$) [27,31], which are generally recognized as the best estimations for ϕ_c of overlapping spheres. This strongly indicates the accuracy of the present MC simulations and finite-size scaling analysis for determining ϕ_c of overlapping spherocylinders.

B. Percolation threshold

Figure 5 presents the obtained values of ϕ_c of overlapping spherocylinders with α from 0 (i.e., spheres) to 200 (i.e., needlelike particles), using the finite-size scaling scheme illustrated above. It can be seen that ϕ_c possesses a maximal value at $\alpha = 0$ (i.e., $\phi_c = 0.2896$), which indicates that overlapping spheres are more difficult to percolate than elongated spherocylinders. Also, ϕ_c is a monotonic decreasing function on α. Such trend is in excellent agreement with that for monodisperse or polydisperse systems of elongated particles reported in the literature [11,14–19]. The numerical values of ϕ_c are provided in Table I.

In addition, we compare the present results with the rigorous theoretical bounds for the percolation threshold of congruent overlapping convex hyperparticles by using a scaling relation [16], in which the lower and upper bounds for the critical volume fraction ϕ_c are expressed as [33]

$$\phi_c = \begin{cases} 1 - e^{(-1/V_{\mathrm{dex}})} & \text{the lower bound} \\ 1 - e^{(-2.7344/V_{\mathrm{dex}})} & \text{the upper bound} \end{cases}, \tag{4}$$

where V_{dex} is the dimensionless excluded volume of the particle defined as the ratio of the excluded volume V_{ex} to the volume V of the particle. V_{dex} for a spherocylinder is given

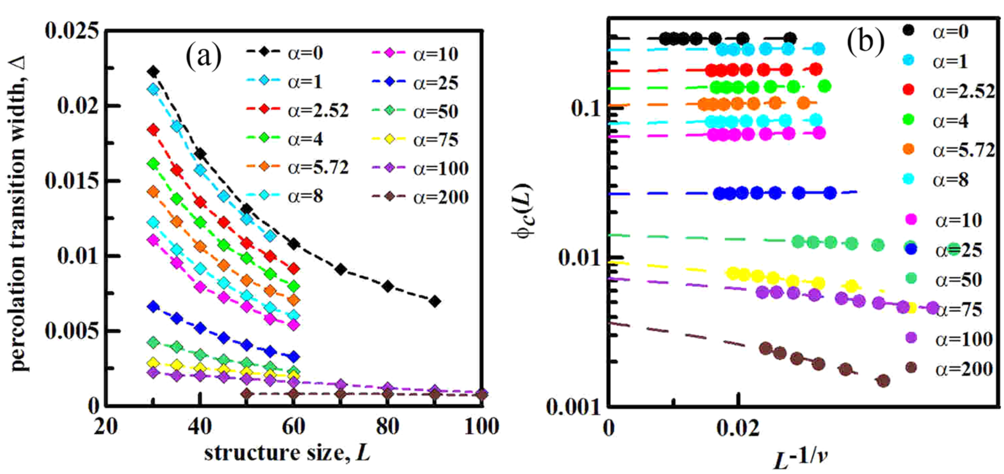

FIG. 4. (a) The percolation transition width Δ for different α as a function of system size L. (b) The effective percolation threshold $\phi_c(L)$ for different α as a function of $L^{-1/\nu}$, with linear fits to the data.

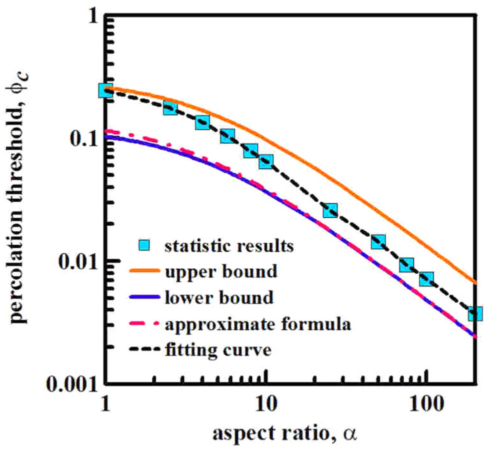

FIG. 5. The percolation threshold ϕ_c for different α. The cubic symbols are the present MC simulation results, the solid lines are theoretical bounds for the percolation threshold of congruent overlapping spherocylinders derived by Torquato and Jiao [16], and the dashed red line is the approximate solution for the percolation threshold reported by Chatterjee [11].

by [34]

$$V_{\mathrm{dex}} = \frac{V_{\mathrm{ex}}}{V} = 2 + \frac{6(1+\alpha)(1+0.5\alpha)}{(1+1.5\alpha)}. \tag{5}$$

Figure 5 clearly shows that our results lie within the rigorous bounds, which further indicates that the present MC simulations and finite-size scaling analysis generate accurate estimates of ϕ_c for a wide range of α. Also, for relatively small aspect ratios (e.g., $\alpha < 25$), our results are close to the upper bound, and gradually get close to the lower bound with increasing α values (see the detailed values of Table I).

We also compare the present results of ϕ_c with corresponding values obtained from an analytical approximation recently proposed by Chatterjee [11,35], i.e.,

$$\phi_c = 1 - e^{\left(\frac{-1}{V_{\mathrm{dex}}-1}\right)}. \tag{6}$$

Figure 5 shows that compared with the present results, the approximation (6) underestimates ϕ_c for the entire range of α values we studied, and the discrepancy is more pronounced for the smaller α. In fact, the approximation (6) [11] almost coincides with the lower bound (4) [16] and becomes an asymptotically exact lower bound in the limit $\alpha \to \infty$. In particular, V_{dex} for the sphere has the smallest value equivalent to 8, and V_{dex} for a spherocylinder is a monotonic increase function of α (see Fig. 5 in [34]), so that $V_{\mathrm{dex}} \gg 1$ as α becomes large.

C. Empirical approximation of percolation threshold

Here, we propose an empirical approximation for ϕ_c in which the exponent explicitly depends both on the dimensionless excluded volume and the aspect ratio of the particles, i.e.,

$$\phi_c = 1 - e^{[-C(\alpha)/V_{\mathrm{dex}}]}, \tag{7}$$

where the numerator in the exponent is determined from our numerical results as follows:

$$C(\alpha) = 1 + (0.136\,169\alpha + 0.165\,568)^{-0.3235}. \tag{8}$$

TABLE I. Percolation threshold ϕ_c derived from MC simulations for congruent overlapping spherocylinders with $R_{\mathrm{eq}} = 1.0$. The rigorous bounds for ϕ_c computed by Eq. (4), where the superscripts L and U denote the lower and upper bounds, respectively.

α	R_{eq}	D	H	ϕ_c (MC simulation)	ϕ_c (bounds)
0	1.0	2	0	0.2896 ± 0.0007	$0.2895^{(U)}$ $0.1175^{(L)}$
1.0	1.0	1.473612599	1.473612599	0.2439 ± 0.0002	$0.2571^{(U)}$ $0.1029^{(L)}$
2.5222	1.0	1.187034119	2.993700048	0.1763 ± 0.0002	$0.2039^{(U)}$ $0.0800^{(L)}$
4.0	1.0	1.045515917	4.182063669	0.1345 ± 0.0001	$0.1681^{(U)}$ $0.06509^{(L)}$
5.7232	1.0	0.941533212	5.388582877	0.1039 ± 0.0001	$0.1391^{(U)}$ $0.05331^{(L)}$
8.0	1.0	0.850580741	6.804645925	0.07862 ± 0.0002	$0.1131^{(U)}$ $0.04296^{(L)}$
10.0	1.0	0.793700526	7.93700526	0.06418 ± 0.0002	$0.09716^{(U)}$ $0.03669^{(L)}$
25.0	1.0	0.592301846	14.80754614	0.02595 ± 0.00004	$0.04708^{(U)}$ $0.01748^{(L)}$
50.0	1.0	0.472163196	23.60815979	0.01440 ± 0.00008	$0.02530^{(U)}$ $0.009329^{(L)}$
75.0	1.0	0.413077343	30.98080074	0.009317 ± 0.00008	$0.01730^{(U)}$ $0.006362^{(L)}$
100.0	1.0	0.375581634	37.55816336	0.007156 ± 0.00005	$0.01314^{(U)}$ $0.004826^{(L)}$
200.0	1.0	0.298429096	59.68581926	0.003724 ± 0.00009	$0.006701^{(U)}$ $0.002455^{(L)}$

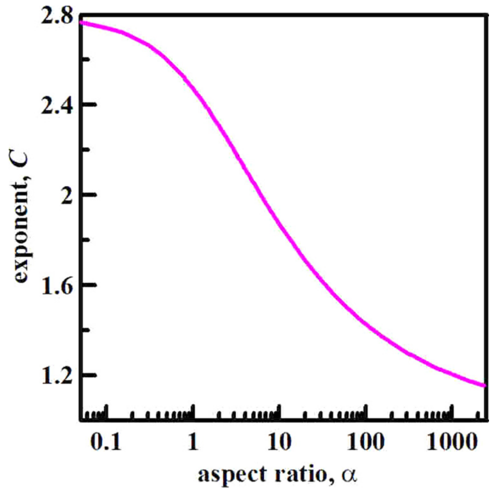

FIG. 6. The effect of aspect ratios α on the exponent C in the proposed theoretical model.

In other words, we do not assume the exponent in Eq. (7) as a fixed constant used in previous studies [11,16], but consider it as a power function of α, as shown in Eq. (8). Interestingly, we find that the values of C for all α in $[0,\infty)$ lie within the interval [1.0, 2.7892] (see Fig. 6), which are consistent with the rigorous bounds (4) [16], although the maximal value of C ($C = 2.7892$) slightly exceeds the exponent (2.7344) of the upper bound shown in Eq. (4). Moreover, our results also extend the ranges of C values which have been previously reported to lie between 1.4 and 2.7 for congruent overlapping particles [2,13,15,20,26].

To further validate our empirical approximation (7), we compare the ϕ_c values obtained using (7) with the numerical and experimental results reported by Mutiso and coworkers [36,37] and with the numerical results obtained by Schilling *et al.* [19]. Figure 7(a) shows the experimental results associated with the silver nanowire-polystyrene composites where the nanowires are regarded as congruent straight rods due to the nature of their narrow size dispersity [37]. It can be seen in Fig. 7(a) that our empirical approximations are in excellent agreement with the corresponding numerical and experimental results for monodisperse rods with finite α from 8 to 100 (over a middle range of α). However, we note that in the experimental system, the particles are not fully penetrable and possess a hard core. Interestingly, in our simulations of the overlapping spherocylinder system containing a large number of particles, the majority of the particles in the system-spanning cluster only contain small regions of overlap with neighboring particles, which results in the reasonable estimates of percolation threshold for the experimental system, for which the overlap between particles is also small. A more accurate treatment of the experimental system is to explicitly consider the hard-core soft-shell model of the particles in the simulation, and to explicitly consider the exclusion volume effect in the empirical formulation.

Figure 7(b) shows the quantitative comparison of our empirical approximations with the numerical results for monodisperse overlapping rods with α from 0 (sphere) to $\alpha = 2000$ (the needle limit) obtained by Schilling *et al.* [19]. Excellent agreement between our empirical approximations and the simulation results for all α in [0, 2000] is observed. These comparisons clearly indicate that our theoretical model can accurately predict the percolation threshold of overlapping spherocylinders with a wide range of aspect ratios, i.e., from 0 to 2000. It is also reasonable to expect that (7) can also provide good estimates of ϕ_c in the limit $\alpha \to \infty$.

D. Effect of particle size

We further investigate the effect of particle size on the percolation threshold. As mentioned above, the size of spherocylinders is characterized by the equivalent sphere radius R_{eq}. Without loss of generality, we select $R_{\mathrm{eq}} = 0.1$, 1.0, 10, and 100, of monodisperse spherocylinders with the same aspect ratio of $\alpha = 8.0$, for our numerical studies. Applying similar MC simulations and finite-size scaling analysis described before (see Figs. 8 and 9), we obtain the percolation threshold ϕ_c and the correlation-length critical exponent ν for different R_{eq} under the same α, as shown in Table II. It can be clearly seen that for different R_{eq}, ϕ_c and ν are insensitive to the

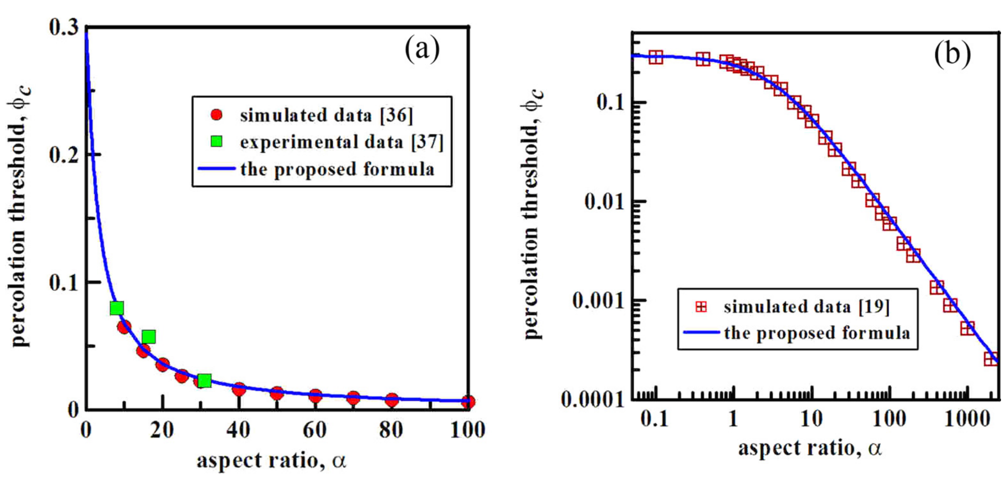

FIG. 7. Comparisons of the proposed empirical approximation with (a) the numerical and experimental results from Mutiso and coworkers [36,37], and with (b) the numerical results from Schilling *et al.* [19].

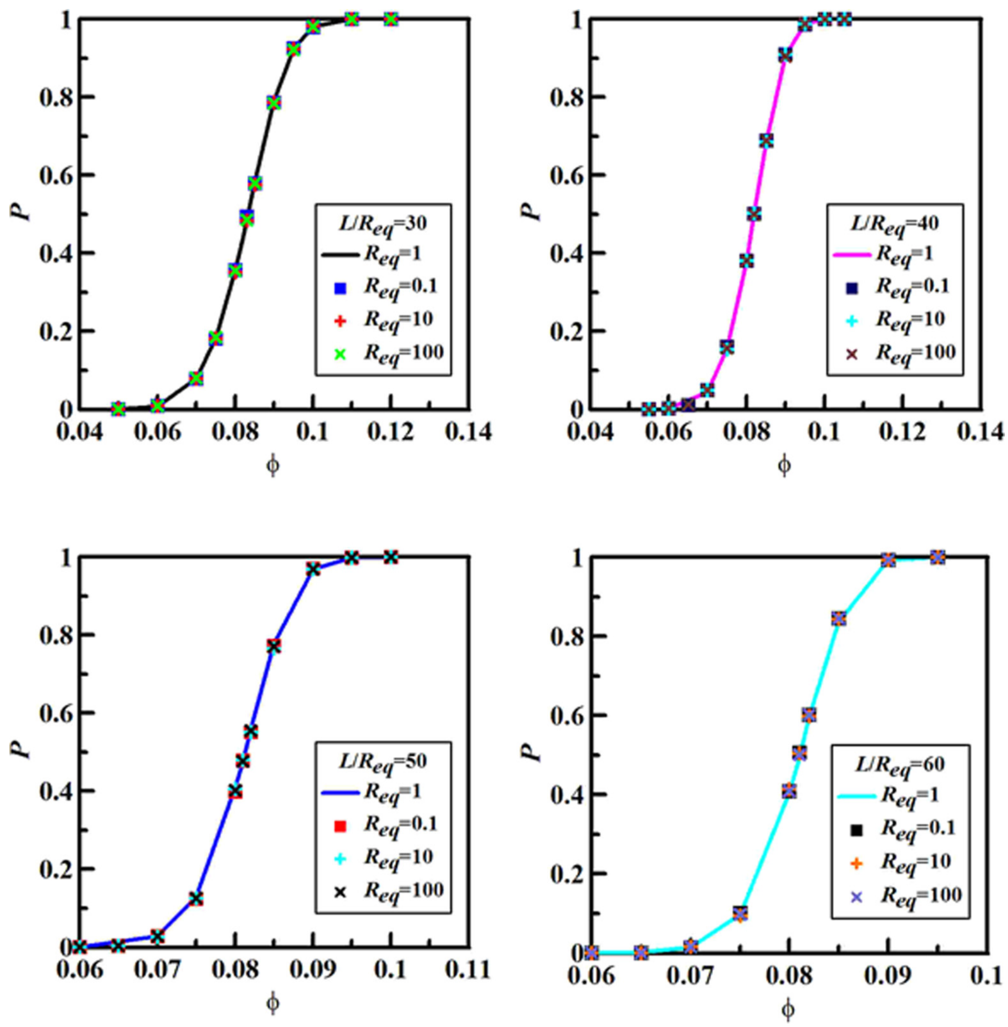

FIG. 8. Percolation probability $P(\phi,L)$ versus ϕ for different R_{eq} and system sizes of L. The parameters of the particles are $\alpha = 8.0$.

particle size, which is consistent with the results for polydisperse spherocylinder systems with different particle size distributions [17,18]. These results suggest that the percolation threshold possesses a universal behavior dependent only on the aspect ratio but not particle size.

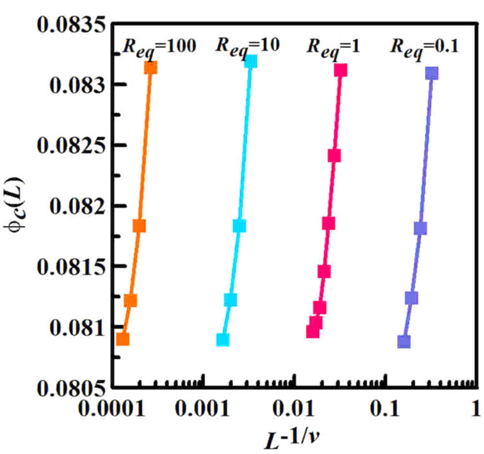

FIG. 9. The effective percolation threshold $\phi_c(L)$ as a function of $L^{-1/\nu}$ for different R_{eq}, with accompanying linear fits to the data.

IV. CONCLUSIONS AND DISCUSSION

In summary, we have presented a comprehensive finite-size scaling analysis of the continuum percolation of randomly orientated congruent overlapping spherocylinders. The percolation threshold ϕ_c, percolation transition width Δ, and correlation-length critical exponent ν for spherocylinders with α in [0, 200] are determined with a high degree of accuracy via extensive Monte Carlo simulations and finite-size scaling analysis. Moreover, a generalized excluded-volume percolation model with an exponent explicitly depending on aspect ratios is proposed that can accurately predict ϕ_c of overlapping spherocylinders with arbitrary aspect ratios α in $[0,\infty)$, which improves upon previous analytical approximations and has validated using available numerical and experimental data for spherocylinders with an aspect ratio up to 2000. We find that ϕ_c is a universal monotonic decreasing function of α and is independent of the effective particle size.

These results suggest a general procedure for constructing an approximation for ϕ_c of nonspherical particles. Specifically,

TABLE II. Percolation threshold ϕ_c and correlation-length critical exponent ν for different R_{eq} with the same $\alpha = 8.0$.

R_{eq}	0.1	1	10	100
ϕ_c	0.07867 ± 0.00001	0.07862 ± 0.00002	0.07849 ± 0.00001	0.07864 ± 0.00001
ν	0.9718 ± 0.0001	0.9868 ± 0.0001	0.9976 ± 0.0001	0.9720 ± 0.0001

the exponent in the approximation is expected to include both a dimensionless excluded-volume term (denominator) and a shape-dependent numerator, as a function of the key geometrical parameter characterizing the nonspherical shape. Our results of ϕ_c and the empirical approximation (7) provide robust and convenient guidance for composites design and evaluation. In future work, we will extend the generalized excluded-volume model to study the physical properties of composites, and discuss how the physical properties are affected by the percolation threshold. In addition, it is also interesting to investigate the effect of chirality on continuum percolation by generalizing the hard helix model for self-assembly studied in Ref. [38].

ACKNOWLEDGMENTS

The authors acknowledge financial support from National Natural Science Foundation of China (Grants No. 11402076 and No. 51679078), Natural Science Foundation for Jiangsu Province (Grant No. BK20130841), China Postdoctoral Science Foundation (Grants No. 2014M560385 and No. 2015T80493), the Open Research Funds for State Key Laboratory of High Performance Civil Engineering Materials (Grant No. 2015CEM004), the Open Research Funds for State Key Laboratory of Simulation and Regulation of Water Cycle in River Basin (Grants No. IWHR-SKL-201511 and No. 2016TS09), and the Fundamental Research Funds for the Central Universities (Grant No. 2016B06314).

[1] S. Torquato, *Random Heterogeneous Materials: Microstructure and Macroscopic Properties* (Springer-Verlag, New York, 2002).
[2] I. Balberg, Phys. Rev. B **31**, 4053 (1985); **33**, 3618 (1986); Phys. Rev. Lett. **59**, 1305 (1987).
[3] C. W. Nan, Y. Shen, and J. Ma, Annu. Rev. Mater. Res. **40**, 131 (2010).
[4] A. V. Kyrylyuk and P. van der Schoot, Proc. Natl. Acad. Sci. U. S. A. **105**, 8221 (2008).
[5] Y. S. Cho, J. S. Lee, H. J. Herrmann, and B. Kahng, Phys. Rev. Lett. **116**, 025701 (2016).
[6] G. Lemoult, L. Shi, K. Avila, S. V. Jalikop, M. Avila, and B. Hof, Nat. Phys. **12**, 254 (2016).
[7] M. A. Miller and D. Frenkel, Phys. Rev. Lett. **90**, 135702 (2003).
[8] G. Lois, J. Blawzdziewicz, and C. S. O'Hern, Phys. Rev. Lett. **102**, 015702 (2009).
[9] S. Torquato, J. Chem. Phys. **136**, 054106 (2012).
[10] T. Schilling, S. Jungblut, and M. A. Miller, Phys. Rev. Lett. **98**, 108303 (2007).
[11] A. P. Chatterjee, J. Phys.: Condens. Matter **20**, 255250 (2008); **27**, 375302 (2015).
[12] C. Y. Zhang, X. L. Jian, and W. Lu, Soft Matter **11**, 1362 (2015).
[13] A. L. R. Bug, S. A. Safran, and I. Webman, Phys. Rev. Lett. **54**, 1412 (1985).
[14] R. H. J. Otten and P. van der Schoot, Phys. Rev. Lett. **103**, 225704 (2009); J. Chem. Phys. **134**, 094902 (2011).
[15] A. Coniglio, U. De Angelis, and A. Forlani, J. Phys. A **10**, 1123 (1977).
[16] S. Torquato and Y. Jiao, J. Chem. Phys. **137**, 074106 (2012); Phys. Rev. E **87**, 022111 (2013).
[17] H. Meyer, P. van der Schoot, and T. Schilling, J. Chem. Phys. **143**, 044901 (2015).
[18] B. Nigro, C. Grimaldi, P. Ryser, A. P. Chatterjee, and P. van der Schoot, Phys. Rev. Lett. **110**, 015701 (2013).
[19] T. Schilling, M. A. Miller, and P. van der Schoot, EPL **111**, 56004 (2015).
[20] I. Balberg, N. Binenbaum, and N. Wagner, Phys. Rev. Lett. **52**, 1465 (1984).
[21] J. Li and S. L. Zhang, Phys. Rev. E **80**, 040104 (2009).
[22] D. R. Stevens, E. W. Skau, L. N. Downen, M. P. Roman, and L. I. Clarke, Phys. Rev. E **84**, 021126 (2011).
[23] J. Li and M. Ostling, Phys. Rev. E **88**, 012101 (2013).
[24] E. J. Garboczi, K. A. Snyder, J. F. Douglas, and M. F. Thorpe, Phys. Rev. E **52**, 819 (1995).
[25] W. X. Xu, H. Wang, Y. Z. Niu, and J. T. Bai, J. Chem. Phys. **144**, 014703 (2016).
[26] Y. B. Yi and A. M. Sastry, Phys. Rev. E **66**, 066130 (2002); Proc. R. Soc. A **460**, 2353 (2004).
[27] M. E. J. Newman and R. M. Ziff, Phys. Rev. Lett. **85**, 4104 (2000); Phys. Rev. E **64**, 016706 (2001).
[28] F. Radicchi and C. Castellano, Nat. Commun. **6**, 10196 (2015).
[29] M. D. Rintoul and S. Torquato, J. Phys. A: Math. Gen. **30**, L585 (1997).
[30] N. Araújo, P. Grassberger, B. Kahng, K. J. Schrenk, and R. M. Ziff, Eur. Phys. J. Spec. Top. **223**, 2307 (2014).
[31] C. D. Lorenz and R. M. Ziff, J. Chem. Phys. **114**, 3659 (2001).
[32] B. Everitt, *The Cambridge Dictionary of Statistics* (Cambridge University Press, New York, 1998).
[33] Torquato and Jiao [16] characterized the percolation threshold as the critical reduced density η_c, according to the relation of $\phi_c = 1 - e^{(-\eta c)}$ [2], the rigorous bounds for the critical volume fraction ϕ_c of monodisperse soft convex particles in three-dimensional space can be rewritten as Eq. (4).
[34] W. X. Xu, G. Q. Yang, P. Lan, and H. F. Ma, CMC Comput. Mater. Continua (unpublished).

[35] z_p [Eq. (8)] in the recent paper reported by Chatterjee [11] is actually equivalent to the dimensionless excluded volume V_{dex} of the spherocylinder. Note that η [Eq. (2)] formulated in [11] is essentially the reduced density rather than the volume fraction of overlapping spherocylinders.

[36] R. M. Mutiso, M. C. Sherrott, J. Li, and K. I. Winey, Phys. Rev. B **86**, 214306 (2012).

[37] S. I. White, R. M. Mutiso, P. M. Vora, D. Jahnke, S. Hsu, J. M. Kikkawa, J. Li, J. E. Fischer, and K. I. Winey, Adv. Funct. Mater. **20**, 2709 (2010).

[38] H. B. Kolli, E. Frezza, G. Cinacchi, A. Ferrarini, A. Giacometti, T. S. Hudson, C. De Michele, and F. Sciortino, Soft Matter **10**, 8171 (2014).